

## RESEARCH LETTER

10.1002/2013GL058729

## Key Points:

- Our results have implications for subduction erosion
- A major velocity discontinuity is detected beneath the middle continental slope
- Possible gravitational collapse of the outermost fore-arc block off north Chile

## Supporting Information:

- Readme
- Supplementary Text

## Correspondence to:

E. Contreras-Reyes,  
econtreras@dgf.uchile.cl

## Citation:

Contreras-Reyes, E., J. Becerra, H. Kopp, C. Reichert, and J. Díaz-Naveas (2014), Seismic structure of the north-central Chilean convergent margin: Subduction erosion of a paleomagmatic arc, *Geophys. Res. Lett.*, *41*, 1523–1529, doi:10.1002/2013GL058729.

Received 25 NOV 2013

Accepted 14 FEB 2014

Accepted article online 18 FEB 2014

Published online 11 MAR 2014

## Seismic structure of the north-central Chilean convergent margin: Subduction erosion of a paleomagmatic arc

Eduardo Contreras-Reyes<sup>1</sup>, Juan Becerra<sup>2</sup>, Heidrun Kopp<sup>3,4</sup>, Christian Reichert<sup>5</sup>, and Juan Díaz-Naveas<sup>6</sup>

<sup>1</sup>Departamento de Geofísica, Facultad de Ciencias Físicas y Matemáticas, Universidad de Chile, Santiago, Chile,

<sup>2</sup>Departamento de Geología, Facultad de Ciencias Físicas y Matemáticas, Universidad de Chile, Santiago, Chile, <sup>3</sup>GEMAR

Helmholtz Centre for Ocean Research, Kiel, Germany, <sup>4</sup>Christian-Albrechts-Universität zu Kiel, Kiel, Germany, <sup>5</sup>Federal Institute and Natural Resources, Hannover, Germany, <sup>6</sup>Escuela de Ciencias del Mar, Universidad Católica de Valparaíso, Valparaíso, Chile

**Abstract** We study the erosive convergent margin of north-central Chile (at ~31°S) by using high-resolution bathymetric, wide-angle refraction, and multichannel seismic reflection data to derive a detailed tomographic 2-D velocity-depth model. In the overriding plate, our velocity model shows that the lowermost crustal velocities beneath the upper continental slope are 6.0–6.5 km/s, which are interpreted as the continental basement composed by characteristic metamorphic and igneous rocks of the Coastal Cordillera. Beneath the lower and middle continental slope, however, the presence of a zone of reduced velocities (3.5–5.0 km/s) is interpreted as the outermost fore arc composed of volcanic rocks hydrofractured as a result of frontal and basal erosion. At the landward edge of the outermost fore arc, the bathymetric and seismic data provide evidence for the presence of a prominent trenchward dipping normal scarp (~1 km offset), which overlies a strong lateral velocity contrast from ~5.0 to ~6.0 km/s. This pronounced velocity contrast propagates deep into the continental crust, and it resembles a major normal listric fault. We interpret this seismic discontinuity as the volcanic-continental basement contact of the submerged Coastal Cordillera characterized by a gravitational collapse of the outermost fore arc. Subduction erosion has, most likely, caused large-scale crustal thinning and long-term subsidence of the outermost fore arc.

### 1. Introduction

At erosive margins, the overriding plate material is removed, causing the steepening of the trench slope and positioning of the continental or island arc basement close to the trench [e.g., *Clift and Vannucchi*, 2004]. Frontal erosion is one mode of subduction erosion, and it takes place at the tip of the fore arc when topographic features on the incoming oceanic plate collide with the apex of the margin, causing the transport of eroded material to the lowermost slope by debris flow. Subduction erosion also removes material from the base of the overriding fore arc (basal erosion), causing the thinning of the upper plate [e.g., *von Huene and Ranero*, 2003]. Thus, subduction erosion leads to large-scale and long-term margin subsidence and the arcward migration of the trench.

The northern Chilean margin is largely recognized as a convergent margin effected by subduction erosion [e.g., *Rutland*, 1971; *von Huene and Ranero*, 2003; *Clift and Vannucchi*, 2004; *Ranero et al.*, 2006; *Kukowski and Oncken*, 2006]. Here the ~38–48 Myr old oceanic Nazca Plate currently subducts at ~6.6 cm/a beneath the South American Plate in an ~N78°E trending direction [*Khazaradze and Klotz*, 2003]. The oceanic plate is covered by a thin layer of pelagic sediment (<100 m), and the trench is, in general, poorly sedimented [*von Huene and Ranero*, 2003; *Clift and Vannucchi*, 2004; *Kukowski and Oncken*, 2006]. The seaward wall of the trench hosts a high-relief horst-graben topography that has been suggested as a cause of abrasion of the base of the overriding fore arc [*von Huene and Ranero*, 2003]. Furthermore, *Rutland* [1971], among other authors, proposed that the northern Chilean margin has been dominated by subduction erosion since the Jurassic based on the eastward migration of the magmatic arc by about 200 km. *Kukowski and Oncken* [2006] estimated an erosion rate of ~100 km<sup>3</sup>/Myr/trench kilometer and an average net crustal loss of approximately 40–45 km<sup>3</sup>/Myr/trench kilometer for northern Chile.

The Juan Fernández Ridge (JFR) is one of the most remarkable bathymetric features of the oceanic Nazca Plate off Chile [e.g., *von Huene et al.*, 1997; *Larsen et al.*, 2002]. The JFR is a hot spot track chain formed by 11

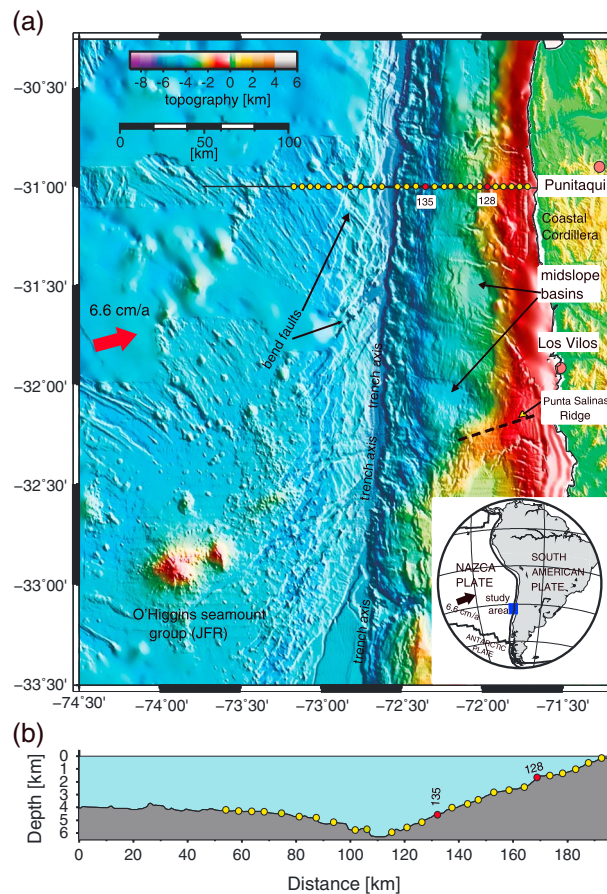


**Figure 1.** (a) Swath bathymetric image of the seafloor off Punitaqui. The incoming O'Higgins seamounts correspond to the easternmost part of the Juan Fernandez Ridge, and they are the next main seamounts to subduct beneath the continental South American Plate. The solid black line denotes the location of the seismic profile, while the red dots indicate the two stations shown in Figures 2a and 2b. (b) Seismic profile and locations of the 26 OBH/OBS stations used in the seismic modeling.

main seamounts, and it has a total length of  $\sim 900$  km. The JFR first collided with the South American continental plate in the north ( $\sim 20^\circ\text{S}$ ) at  $\sim 22$  Ma, and it has progressively migrated southward to the current collision zone located at  $32^\circ\text{--}33^\circ\text{S}$  [Yáñez *et al.*, 2001]. The current ridge-trench collision zone has remained stationary since  $\sim 10$  Ma [Yáñez *et al.*, 2001]. In addition, the JFR behaves as a barrier for trench sediment transport along the trench in the current ridge-trench collision zone separating a poorly sedimented trench to the north from a sediment-flooded trench to the south [e.g., Laursen *et al.*, 2002]. Consequently, the JFR separates a tectonically erosive margin, in the north from an accretionary margin in the south [e.g., von Huene *et al.*, 1997]. Moreover, it is expected that this feature has accelerated the subduction erosion during the ridge-trench collision [Kukowski and Oncken, 2006] as has been reported for the Tonga Trench with the subduction of the Louisville Ridge [i.e., Ballance *et al.*, 1989].

Neotectonic observations [Armijo and Thiele, 1990; DeLouis *et al.*, 1998; Hartley *et al.*, 2000; González *et al.*, 2003] and seismic reflection and bathymetric data [von Huene and Ranero, 2003] indicate east-west extension across the continental region and continental slope in north Chile ( $23\text{--}24^\circ\text{S}$ ). A 2-D velocity-derived porosity model offshore Mejillones Peninsula (north Chile at  $\sim 23.5^\circ\text{S}$ ) was obtained by Sallarès and Ranero [2005] by using wide-angle seismic data. Their results show a progressive reduction in seismic velocities from  $\sim 6.0$  to  $\sim 4.0$  km/s and an increase of rock porosity toward the trench. Hence, the authors proposed that the overriding crust is mainly composed of arc-type igneous basement, where the tip of the margin is probably fluid saturated and disaggregated by fracturation as a consequence of subduction erosion. At depths greater than  $\sim 20$  km, however, low-porosity values were interpreted as little hydrofractured upper plate [Sallarès and Ranero, 2005]. More recent published 2-D velocity-depth models off Tocopilla (north Chile at  $\sim 22^\circ\text{S}$ ) [Contreras-Reyes *et al.*, 2012] and off north-central Chile at  $\sim 32^\circ\text{S}$  [Koulakov *et al.*, 2011; Kopp, 2013] also present a progressive reduction in continental crustal velocities toward the trench. These observations were also attributed to hydrofracturing of the upper plate due to subduction erosion, suggesting that this is a common feature of the northern Chilean margin.

One of the most striking features of the northern Chilean coastal region is the trench-parallel Coastal Cordillera or Coastal Range, which was formed by the exhumation and uplift of a Mesozoic palaeomagmatic arc [e.g., Coira *et al.*, 1982; Charrier *et al.*, 2007]. Underplating at the base of the continental crust inboard of the zone of subduction erosion is the most invoked explanation for the uplift of the Coastal Cordillera [Scheuber *et al.*, 1994; Hartley *et al.*, 2000; Allmendinger and Gonzalez, 2010]. However, subduction erosion will only cause underplating and uplift of the Coastal Cordillera if the eroded material is not subducted to larger depths. Hence, the proposed hypothesis is poorly constrained owing to the scarcity of geophysical data constraining the deep crustal structure below the Coastal Cordillera.

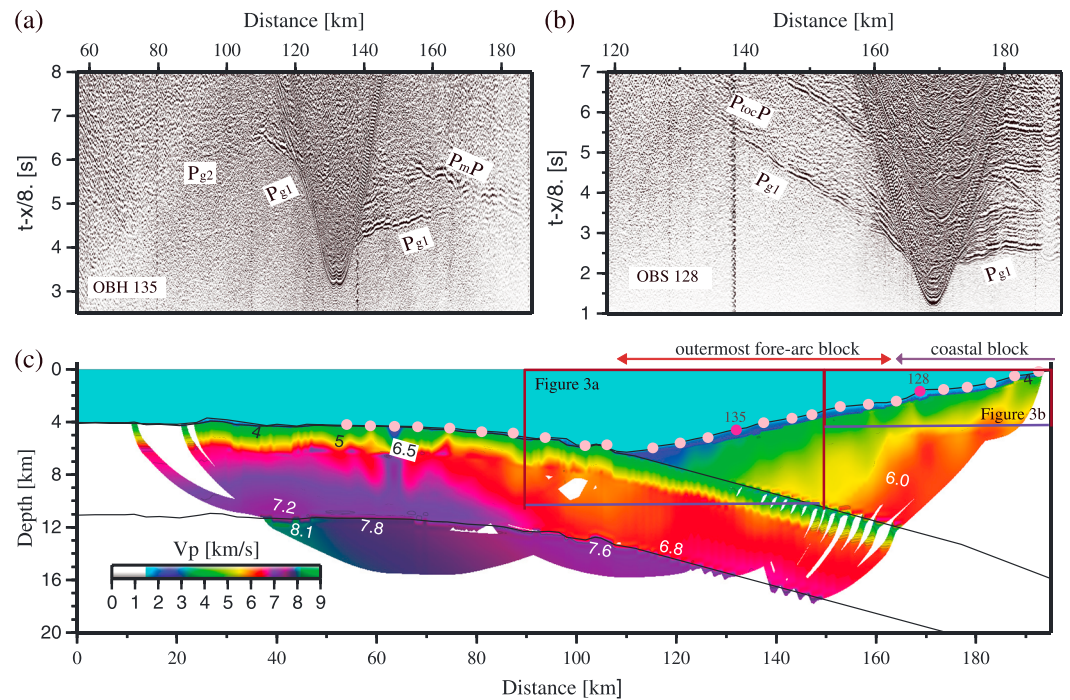


**Figure 2.** Seismic record examples of OBH data with identified travel times: (a) OBH 135 and (b) OBH 128. (c) Two-dimensional final velocity-depth model obtained from joint refraction and reflection tomographic travel time inversion.

In this paper, we present a joint refraction and reflection travel time tomographic approach to derive a detailed 2-D velocity-depth model constrained by high-resolution multichannel seismic reflection and bathymetric data. We present a seismic profile offshore north-central Chile at  $\sim 31^\circ\text{S}$ , and it includes the outer rise region, trench axis, and the submarine fore arc. Our seismic results provide evidence for a velocity discontinuity at the outermost fore arc of the overriding South American continental plate defining a major discontinuity between the inner and outermost fore arcs. The results of this seismic study may offer insights into tectonic evolution and subduction erosion of the continental plate.

## 2. Geophysical Data and Modeling

We analyzed wide-angle seismic refraction and reflection data that were acquired along a single profile located off Punitaqui, north-central Chile, at  $\sim 31^\circ\text{S}$ , supplemented by high-resolution multichannel seismic reflection and swath bathymetric images of the surrounding seafloor [Reichert *et al.*, 2002]. The data were acquired in 2000/2001 onboard the German research vessel *Sonne* [Flueh and Kopp, 2002]. For the seismic experiment, shots were recorded with a total number of 26 ocean bottom seismometers (OBS) and ocean bottom hydrophones (OBH), covering a total length of  $\sim 196$  km (Figure 1). The spacing between the instruments was approximately 5 km. The seismic source was a tuned array of 20 air guns that provided a total volume of 51.2 L, and it was fired at a time interval of 60 s providing an average shot spacing of  $\sim 150$  m. The seismic stations recorded refractions through the overriding plate ( $P_{g1}$ ), reflections from the top of the oceanic crust ( $P_{tocP}$ ), oceanic crustal refractions ( $P_{g2}$ ), Moho wide-angle reflections ( $P_{mP}$ ), and upper mantle refractions ( $P_n$ ) of excellent quality (Figures 2a and 2b). Figure 2b shows an example of record section OBH 128 positioned on the middle-upper continental slope. The data show an abrupt increase landward of apparent  $P_{g1}$  velocities from the middle-upper continental slope transition zone, suggesting important lateral variations.

We used the joint refraction/reflection 2-D tomographic inversion code of Korenaga *et al.* [2000] to derive the seismic velocity-depth model (see supporting information for details). The 2-D velocity-depth model consists of the following units: (1) water, (2) overriding crust, (3) oceanic crust, and (4) upper oceanic mantle. In order to derive the seismic velocities of the overriding crust, and the top of the oceanic basement, we jointly inverted refracting ( $P_{g1}$ ) and reflecting ( $P_{tocP}$ ) phases. The overriding crust velocities and interplate boundary obtained from the tomographic inversion were then held fixed in the following iterative inversions. The oceanic crustal

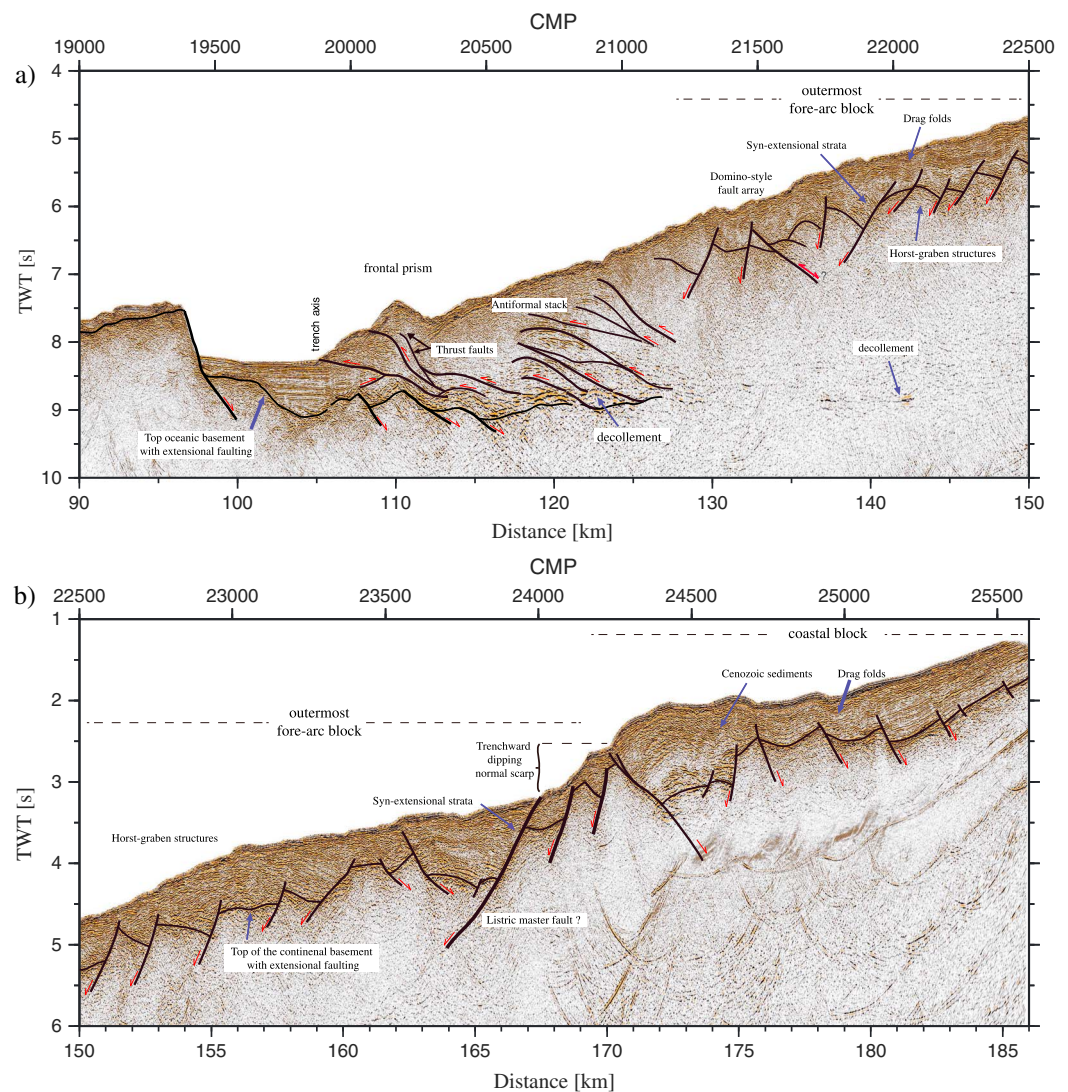


**Figure 3.** Poststack time migration and interpretation of the (a) trench and seaward part of the outermost fore-arc block (b) landward part of the outermost fore-arc block and seaward part of the Coastal Block (see more details in the supporting information).

velocities and Moho depths were inverted using *Pg2* and *PmP* phases. Similarly, the oceanic crustal velocities and Moho depths remained fixed for the next step of the inversion, where the upper mantle velocities were derived using oceanic *Pn* phases. The final 2-D velocity-depth model is presented in Figure 2c. See supporting information for reference model, inversion parameters, and model resolution.

### 3. Results

In the oceanic plate, the lower crustal and upper mantle velocities progressively decrease trenchward and present minimum values beneath the outer rise region of ~6.8 and ~7.6 km/s, respectively (Figure 2c). The onset of low crustal and mantle velocities spatially correlates with the presence of pronounced extensional bend faults and large horst and graben topography seen in the high-resolution seismic reflection and bathymetric data (Figure 1, Figure 3a, and supporting information).

In the continental plate, the 2-D velocity-depth model shows the presence of an ~5 km wide wedge-shaped body, with relative low velocities of 2.0–3.5 km/s. Landward of this body, velocities increase continuously from ~3.5 km/s up to ~5.0 km/s within a distance of 50 km (Figure 2c). At ~165 km (beneath the middle-upper slope transition), a strong lateral velocity gradient is detected, from which crustal velocities reach values

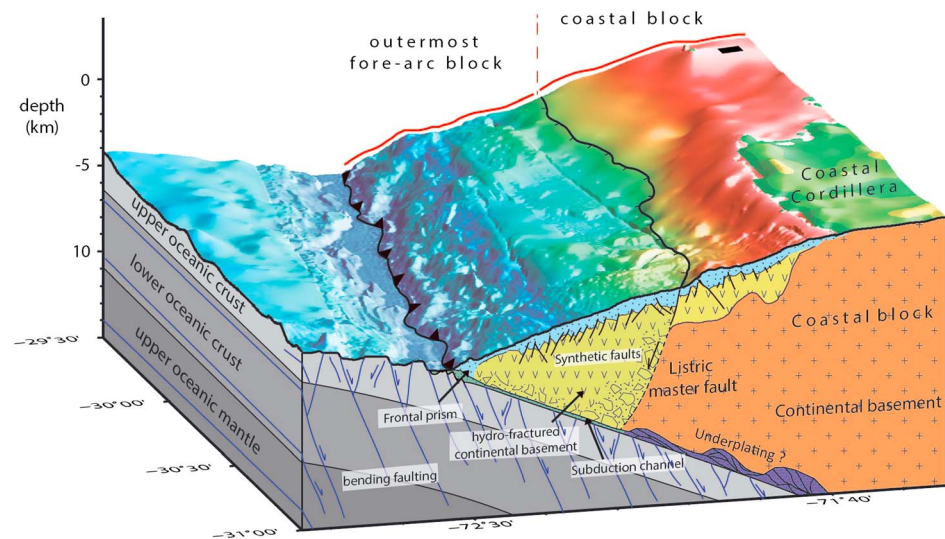


**Figure 4.** Summarized tectonic interpretation (*vertical exaggeration 2:1*). The outermost fore-arc block is composed of volcanic rocks that are largely hydrofractured as a consequence of subduction erosion. The landward limit of the outermost fore-arc block is coincident with the location of the continental slope scarp suggesting subsidence of the outermost fore-arc block. The Coastal Block is composed of igneous and metamorphic rocks that form part of the uplifted Coastal Cordillera.

higher than 6.0 km/s. This remarkable feature presents an abrupt velocity contrast that propagates deep into the continental crust, and it resembles a deep fault dipping trenchward, which spatially correlates with a prominent scarp seen in the multichannel seismic reflection data (Figure 3b). To check the resolution and stability of this feature on the final tomographic model, we conducted a test with different initial 2-D velocity-depth models. The results shown in the supporting information provide evidence that the data coverage yields a sufficiently high resolution to solve the location and shape of the seismic discontinuity.

#### 4. Discussion

Figure 4 shows our interpretation of the north-central Chilean convergent margin based on our 2-D velocity-depth model constrained with high-resolution bathymetric and multichannel seismic reflection data. Hereafter, we will refer to the unit located between the trench and middle-upper slope transition (~165 km) as the outermost fore-arc block, and we will refer to the unit between the middle-upper slope and the Coastal Cordillera as the Coastal Block (Figure 4).

The trench axis is filled with a thin sediment layer likely composed of a mixture of pelagic sediment, turbidites, and slope debris rich in water. A part of the trench fill is further incorporated to the subduction channel, and the rest is added to the toe of the overriding plate to form the frontal prism. We interpret the ~5 km wide wedge-shaped body, with low velocities of 2.0–3.5 km/s as the frontal prism at the base of the continental slope (Figures 2c and 4). The landward edge of the frontal prism of the offscraped material is characterized by a strong reflection that separates a thin surface layer from the deeper, higher-velocity rocks (Figure 3a and supporting information).

Extensional faults are imaged into the slope debris/sediment layer and upper part of the continental crust (Figure 3). Seismic velocities decrease progressively from ~5.0 to ~3.5 km/s from the outermost fore-arc-coastal block transition zone up to the landward edge of the frontal prism (Figure 2c). These velocities might correspond to volcanic rocks of a Mesozoic magmatic arc that currently form part of the outermost fore-arc block. The progressive decrease in seismic velocities trenchward is accompanied by a thinning of the outermost fore-arc block, and it is likely related to the combined effect of an increase in rock fracturation, porosity, and hydration. Reduced continental crustal velocities in the frontal part of the margin have also been observed farther north off Chile at ~23.5°S [Sallarès and Ranero, 2005] and at ~22°S [Contreras-Reyes *et al.*, 2012]. Furthermore, von Huene and Ranero [2003] proposed that the frontal part of the northern Chilean margin is highly permeated by fluids from underthrusting debris that hydrofracture the base of the overriding plate and reduce interplate friction.

At the outermost fore-arc-coastal block transition zone, a large fault scarp with a height of ~1 km lies above the onset of an abrupt velocity contrast that propagates deep into the continental crust, and it is interpreted as a deep extensional listric fault dipping trenchward. Likely, the seafloor scarp is tectonic related, where the associated master fault is the interpreted crustal discontinuity at the landward edge of the outermost fore-arc block (Figure 4). The interpreted master fault has a relative low angle of ~30°–40°, which is typical for listric faults in collapse-extensional environments [e.g., Imber *et al.*, 2003]. A plausible mechanism explaining the subsidence of the outermost fore-arc block is the thinning of the outermost fore-arc crust enhanced by subduction erosion [e.g., von Huene and Ranero, 2003; Sallarès and Ranero, 2005]. The collision and subduction of high-relief horst-graben structures and the JFR frontally and basally remove the material from the front and the base of the overriding plate, leading to large-scale crustal thinning and long-term subsidence of the outermost fore-arc block.

The increase in seismic velocities landward of the outermost fore-arc block suggests that subduction erosion is less intense here, and the continental crust is not much hydrofractured. The Coastal Block has lowermost crustal velocities of 6.0–6.5 km/s, which are interpreted as the continental basement composed by metamorphic and igneous rocks of the Coastal Cordillera [Servicio Nacional de Geología y Minería de Chile (SERNAGEOMIN), 2003]. In the eastern and central part of the upper slope, extensional landward dipping faults cut the basement and slope sediment sequences and generate drag folds and little landward dipping scarps (Figure 3b). Another important structural feature shown in the seismic reflection data is the uplifted Coastal Block. Geological onshore units of the Coastal Cordillera in the study region are Upper Cretaceous(?) to Cenozoic marine and continental sediments and the continental basement, which is composed by the Paleozoic metamorphic complex and Triassic-Jurassic intrusives [SERNAGEOMIN, 2003].

Assuming that the same geological units form part of the submerged Coastal Cordillera, the structural differences between the outermost fore-arc and coastal blocks might be related to the rheology of the continental basement. The submarine fore arc can be divided into a relative weak subsided outermost fore-arc block, characterized by an active and highly fractured extensional system and a relative strong coastal uplifted block (Figure 4). The removed material from the relative weak outermost fore-arc block is further subducted, and it is possibly stacked and highly compacted beneath the more rigid Coastal Block allowing its uplift. This mechanism is consistent with the subsidence and uplift of the outermost fore arc and coastal blocks, respectively.

#### Acknowledgments

This work was supported by the Chilean National Science Foundation (FONDECYT) project 1130004. Juan Becerra gratefully acknowledges a scholarship granted by the Chilean National Science Cooperation (CONICYT). Helpful comments provided by Daniel Carrizo are greatly appreciated. We would also like to thank Harm van Avendonk, an anonymous reviewer, and the Editor Andrew Newman for their careful reviews of the manuscript.

The Editor thanks Eli Silver and an anonymous reviewer for their assistance in evaluating this paper.

#### References

- Allmendinger, R., and G. Gonzalez (2010), Neogene to Quaternary tectonics of the Coastal Cordillera, northern Chile, *Tectonophysics*, *495*, 93–110.
- Armijo, R., and R. Thiele (1990), Active faulting in northern Chile: Ramp stacking and lateral decoupling along a subduction plate boundary?, *Earth Planet. Sci. Lett.*, *98*, 40–61.
- Ballance, P. F., D. W. Scholl, T. L. Vallier, and R. H. Herzer (1989), Subduction of a Late Cretaceous seamount of the Louisville Ridge at the Tonga Trench: A model of normal and accelerated tectonic erosion, *Tectonics*, *8*, 953–962.
- Charrier, R., L. Pinto, and M. P. Rodríguez (2007), Tectono-stratigraphic evolution of the Andean orogen in Chile, in *Geology of Chile*, Special Publication, edited by W. Gibbons and T. Moreno, chap. 3, pp. 21–116, The Geological Society, London.
- Clift, P., and P. Vannucchi (2004), Controls on tectonic accretion versus erosion in subduction zones: Implications for the origin and recycling of the continental crust, *Rev. Geophys.*, *42*, RG2001, doi:10.1029/2003RG000127.
- Coira, B., J. Davidson, C. Mpodozis, and V. A. Ramos (1982), Tectonic and magmatic evolution of the Andes of northern Argentina and Chile, *Earth Sci. Rev.*, *18*, 303–332, doi:10.1016/0012-8252(82)90042-3.
- Contreras-Reyes, E., J. Jara, I. Grevemeyer, S. Ruiz, and D. Carrizo (2012), Abrupt change in the dip of the subducting plate beneath north Chile, *Nat. Geosci.*, *5*(5), 342–345, doi:10.1038/ngeo1447.
- Delouis, B., H. Philip, L. Dorbath, and A. Cisternas (1998), Recent crustal deformation in the Antofagasta region (northern Chile) and the subduction process, *Geophys. J. Int.*, *132*, 302–338.
- Flueh, E. R., and H. Kopp (2002), SPOC (SONNE Cruise SO-161 Leg 1 and 4), Subduction Processes off Chile, *Geomar Rep.* *102*, Geomar, Kiel, Germany.
- González, G., J. Cembrano, D. Carrizo, A. Macci, and H. Schneider (2003), The link between forearc tectonics and Pliocene Quaternary deformation of the Coastal Cordillera, northern Chile, *J. South Am. Earth Sci.*, *16*, 321–342.
- Hartley, A. J., G. May, G. Chong, P. Turner, S. J. Kape, and E. J. Jolley (2000), Development of a continental forearc: A Cenozoic example from the central Andes, northern Chile, *Geology*, *28*, 331–334.
- Imber, J., C. Childs, P. A. R. Nell, J. J. Walsh, D. Hodgetts, and S. Flint (2003), Hanging wall fault kinematics and footwall collapse in listric growth fault systems, *J. Struct. Geol.*, *25*, 197–208.
- Khazaradze, G., and J. Klotz (2003), Short- and long-term effects of GPS measured crustal deformation rates along the south central Andes, *J. Geophys. Res.*, *108*(B6), 2289, doi:10.1029/2002JB001879.
- Kopp, H. (2013), Invited review paper: The control of subduction zone structural complexity and geometry on margin segmentation and seismicity, *Tectonophysics*, *589*, 1–16, doi:10.1016/j.tecto.2012.12.037.
- Korenaga, J., W. S. Holbrook, G. M. Kent, P. B. Kelemen, R. S. Detrick, H.-C. Larsen, J. R. Hopper, and T. Dahl-Jensen (2000), Crustal structure the southeast Greenland margin from joint refraction and reflection seismic tomography, *J. Geophys. Res.*, *105*, 21,591–21,614, doi:10.1029/2000JB900188.
- Koulakov, I., H. Kopp, and T. Stupina (2011), Finding a realistic velocity distribution based on iterating forward modelling and tomographic inversion, *Geophys. J. Int.*, *186*, 349–358, doi:10.1111/j.1365-246X.2011.05034.x.

- Kukowski, N., and O. Oncken (2006), Subduction erosion: The "normal" mode of forearc material transfer along the Chilean margin?, in *The Andes: Active Subduction Orogeny*, *Frontiers in Earth Sciences*, vol. 3, edited by O. Oncken et al., pp. 217–236, Springer, Berlin.
- Laursen, J., D. W. Scholl, and R. von Huene (2002), Neotectonic deformation of the central Chile margin: Deepwater forearc basin formation in response to hot spot ridge and seamount subduction, *Tectonics*, *21*(5), 1038, doi:10.1029/2001TC901023.
- Ranero, C. R., R. von Huene, W. Weinrebe, and C. Reichert (2006), Tectonic processes along the Chile convergent margin, in *The Andes-Active Subduction Orogeny*, *Frontiers in Earth Sciences*, edited by O. Oncken et al., pp. 91–121, Springer, Berlin.
- Reichert, C., B. Schreckenberger, and the SPOC Team (2002), Fahrtbericht SONNE-Fahrt SO161 Leg 2y3 SPOC, Subduktionsprozesse vor chile-BMBF-Forschungsvorhaben 03G0161A-Valparaiso 16.10.2001- Valparaiso 29.11.2001. fuer Geowis. und Rohstoffe. Bundesanst. Hannover, Germany.
- Rutland, R. W. R. (1971), Andean orogeny and ocean floor spreading, *Nature*, *233*, 252–255.
- Sallarès, V., and C. R. Ranero (2005), Structure and tectonics of the erosional convergent margin off Antofagasta, north Chile (23\_300S), *J. Geophys. Res.*, *110*, B06101, doi:10.1029/2004JB003418.
- Scheuber, E., T. Bogdanic, A. Jensen, and K.-J. Reutter (1994), *Tectonics of the Southern Central Andes*, pp. 121–139, Springer, Berlin.
- SERNAGEOMIN: Chilean Geological and Mining Service (2003), Geologic map of Chile: Digital version, scale 1:1.000.000, Santiago, Chile.
- von Huene, R., and C. R. Ranero (2003), Subduction erosion and basal friction along the sediment-starved convergent margin off Antofagasta, Chile, *J. Geophys. Res.*, *108*(B2), 2079, doi:10.1029/2001JB001569.
- von Huene, R., J. Corvalán, E. R. Flueh, K. Hinz, J. Korstgard, C. R. Ranero, W. Weinrebe, and the CONDOR Scientists (1997), Tectonic Control of the subducting Juan Fernández Ridge on the Andean margin near Valparaíso, Chile, *Tectonics*, *16*, 474–488.
- Yáñez, G., C. R. Ranero, and J. Díaz (2001), Magnetic Anomaly interpretation across the southern central Andes (32°–34°S): The role of the Juan Fernández Ridge in the late Tertiary evolution of the margin, *J. Geophys. Res.*, *106*, 6325–6345.